Enhanced optical forces between coupled resonant metal nanoparticles

Anna S. Zelenina

ICFO–Institut de Ciencies Fotoniques, Mediterranean Technology Park, 08860 Castelldefels (Barcelona), Spain

Romain Quidant*

ICFO–Institut de Ciencies Fotoniques, Mediterranean Technology Park, 08860 Castelldefels (Barcelona), Spain

Manuel Nieto-Vesperinas

ICMM–Instituto de Ciencia de Materiales de Madrid, Consejo Superior de Investigaciones Cientificas, Cantoblanco, 28049 Madrid, Spain

Received December 22, 2006; revised January 25, 2007; accepted February 3, 2007; posted February 7, 2007 (Doc. ID 78361); published April 3, 2007

We investigate numerically the optical forces between noble metal nanoparticles sustaining localized surface plasmon resonances. Our results first point out enhanced binding optical forces compared with dielectric nanoparticles and nonresonant metallic nanoparticles. We also show that under suitable illumination conditions, short-range forces tend to make the nanoparticles cluster, leading to intense and localized hot spots in the interstices. This effect corroborates recent experimental observations of an enhanced Raman signal in trapped metal sphere ensembles. © 2007 Optical Society of America

OCIS codes: 140.7010, 240.5420, 260.3910, 240.0240.

Optical forces induced by light on an object increase with its polarizability and consequently with its dielectric permittivity. It has been shown that metallic particles much smaller than the incident wavelength can be efficiently trapped in a conventional optical trap.[1,2] We have recently investigated how the dispersion of metal nanoparticles (MNPs) can be exploited to either trap or selectively guide them.[3]

In the past, there has been a strong interest in strongly coupled MNPs, in particular for the strong field enhancement they can lead to. Specifically, in two closely spaced MNPs, illuminated by a wave with an electric vector linearly polarized parallel to the particle alignment, the strong surface charges induced across the gap lead to high field enhancements and confinements of interest for reinforcing light-matter interaction,[4,5] and high-resolution near-field imaging and sensing.[6] This geometrical gap effect can be enhanced when the incident wavelength matches the plasmon resonance band of the coupled particles.

Lately, several groups have observed self-clustering of MNPs in a conventional optical trap.[7–9] Svedberg and collaborators[7,8] have shown that such light-induced aggregates lead to a significant enhancement of the Raman field compared with that of uncoupled MNPs. In this Letter, we report on a systematic study of optical forces between MNPs in both far-field and near-field electromagnetic interaction regimes that elucidate previous experimental observations.

The configuration that we consider is sketched in Fig. 1(A). Gold MNPs with a 50 nm diameter are lying on a glass substrate and are illuminated by a polarized plane wave under normal incidence (intensity of 10^{12} W/m^2) from a water superstrate. We look at assemblies of two and three MNPs, characterized by δ, the gap distance between two neighbor MNPs. The model employed to calculate the optical forces makes use of the Green dyadic method and Maxwell's stress tensor.[10] This procedure involves multipolar contributions that cannot be neglected for metal particles of diameter larger than a few tens of nanometers. Also, a surface correction on the Green tensor in a homogeneous medium accounts for the surface contribution.

Since the total forces exerted on a metallic object strongly depend on its scattering efficiency,[3] we first compute the scattering power spectrum for different systems of interest where δ=25 nm. For reference, the scattering of a single MNP is also shown. Results are plotted in Fig. 1(B). For separation distances δ much smaller than the incident wavelength, MNPs interact under the near-field coupling regime through the overlapping of the evanescent fields that tail off from their corresponding metal surfaces. For dimers, illuminated under an incident field polarized along its long axis, this strong interaction leads to coupled resonant modes associated with a broaden-

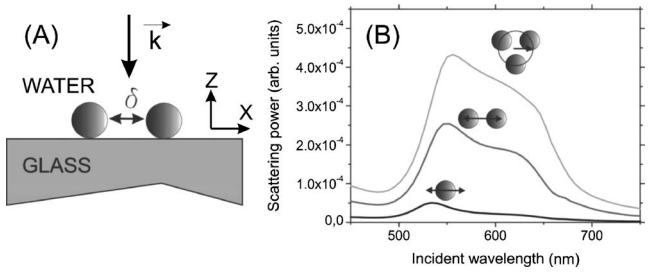

Fig. 1. (A) Optical configuration. (B) Evolution of the scattering efficiency versus wavelength when gold nanospheres (50 nm diameter) agglomerate in dimers and trimers (gap distance δ=25 nm). The arrow marks the polarization of the incident electric vector.

0146-9592/07/091156-3/$15.00

ing, a redshift, and an enhancement of the resonant scattering band compared with a single particle.[11,12] This well-known effect can be understood using a simple dipolar model and considering the compensation of surface polarization charges in the gap space. For the same polarization state, further broadening, enhancement and redshift are observed when adding a third particle to form a hexagonal cell or a chain (not shown).

Figure 2 shows the evolution of the total force experienced by one of the particles of a gold dimer along the X axis as a function of the interparticle distance δ. In the entire study, we do not consider the repulsive Z component of the force since under the illumination configuration we consider the glass substrate would block the MNPs at its surface. Note, however, that all our calculations can be extended away from a surface by considering two incoherent counterpropagating plane waves that would cancel the Z-force contribution. The calculation is performed at both the dimer resonance ($\lambda = 550$ nm) and far away from it ($\lambda = 1064$ nm) so that the actual contribution of the plasmon can be assessed. For the largest separation distances ($\delta > 100$ nm), the curves are characterized by oscillations around the equilibrium position ($F_X = 0$), this X force thus being either attractive or repulsive. These oscillations reported both theoretically[13] and experimentally[14] for dielectric spheres result from the phase relationship between the field scattered and reflected by the two spheres. In the case of metallic spheres, the stronger scattering and reflectivity leads to bigger oscillations compared with those from dielectric objects of the same size (enhancement factor of ~ 20). However, an additional significant increase is expected when the illumination matches the resonance band of the dimer. Indeed, for $\lambda = 550$ nm, the magnitude of the oscillations

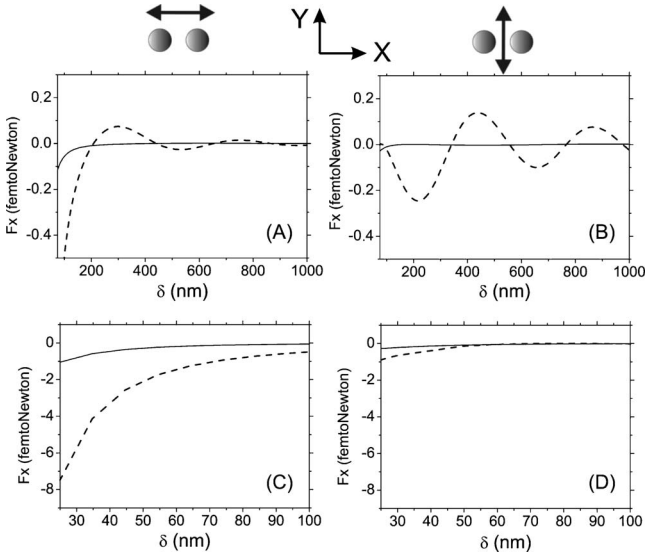

Fig. 2. Evolution of the F_X component of the total force with the gap space δ [(A) and (B) for big δ, (C) and (D) for small δ] on one particle of a gold dimer at its resonance $\lambda = 550$ nm (dashed curve) and away from it $\lambda = 1064$ nm (continuous curve). The double arrow gives the incident linear polarization direction.

grows by a factor of 70 compared with what is observed out of the plasmon band at $\lambda = 1064$ nm. A further effect from the local field enhancement around the particles is the significant increase (by a factor of 7 at $\delta = 25$ nm) of the attraction force between the particles at very short distances [Fig. 2(C)]. Independently of the incidence wavelength, the incident polarization has a dramatic influence on both long- and short-range interaction. For an incident field polarized perpendicularly to the MNPs alignment, we observe that binding optical forces are significantly increased and the binding positions shifted. Inversely, the short-range attraction is considerably reduced. This confirms that the strong attraction observed in Fig. 2(C) relies on the field concentration in between the MNPs.

From the simple case of two interacting gold particles, we now extend our calculations to three particles when aligned ("chain" conformation) and when arranged in a hexagonal network ("trimers" conformation). In both cases, neighboring particles are separated by the same distance δ. We first investigate the trimer configuration for which, instead of a linear polarization, we consider a circularly polarized illumination to render symmetrical the total force on each of the three particles. Under these conditions, the scattering efficiency for $\delta = 25$ nm shows a further redshift and broadening of the plasmon band with respect to the dimer, together with an increase of the maximum scattering magnitude [Fig. 1(B)]. Despite the resonance shift, the system remains resonant at $\lambda = 550$ nm. In Figs. 3(A) and 3(C) the total interparticle force exerted on one particle of the trimer is plotted as a function of δ for both $\lambda = 550$ and 1064 nm. Compared with the dimer case, the introduction of a third particle has two major effects on the force curve. On the one hand, the binding forces at longer distances increase by a factor of 5. Interestingly, the oscillations are also slightly shifted toward shorter δ values. On the other hand, despite the stronger scattering cross section, the maximum force amplitude at $\delta = 25$ nm becomes slightly weaker. This is attributed to a weaker variation of the local field in the gap spaces between the particles since now, at small distances, the field intensity pattern from the three nonaligned particles results in a smaller interaction energy. A different behavior is observed for the chain conformation when illuminated by a field linearly polarized along the particle alignment. Figures 3(B) and 3(D) show no significant modification with respect to the dimer case, and both the binding oscillations and the short-range attraction force are maintained to a similar level.

Previous results indicate optical binding between MNPs preferentially occurs according to specific geometries and is strongly influenced by the illumination conditions (i.e., polarization and wavelength). Nevertheless, in practice, the ability of MNPs to stably organize through optical binding depends on whether the binding well is deep enough to compensate Brownian fluctuations. In Fig. 3(E), the optical potential is plotted for both the dimer and the trimer conformations. The results show that for the incident

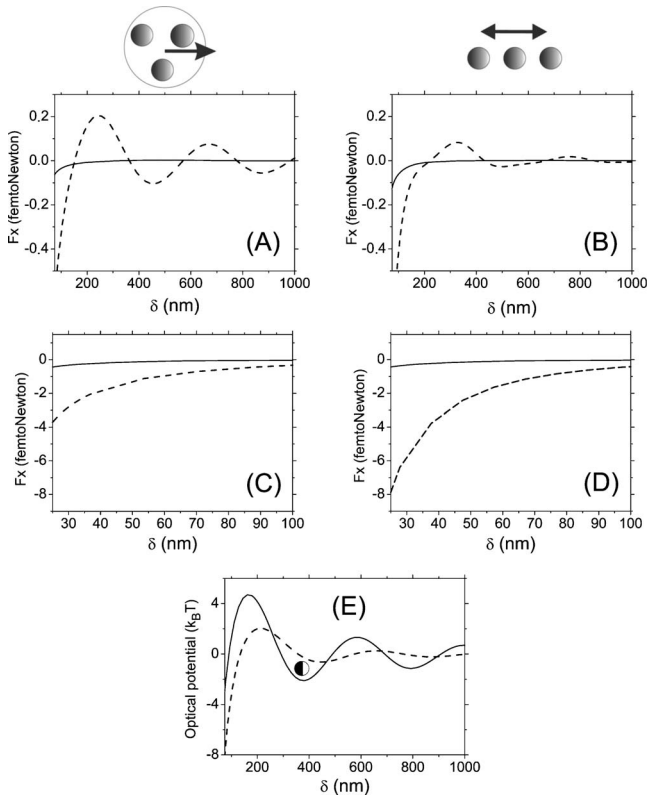

Fig. 3. Evolution of the F_X component of the total force with the gap space δ one particle of a (A) and (C) gold trimer and of a (B) and (D) gold chain both at $\lambda = 550$ nm (dashed curve) and $\lambda = 1064$ nm (continuous curve). (E) Optical potential associated to the force curves in Figs. 2(A) and 3(A) at $\lambda = 550$ nm.

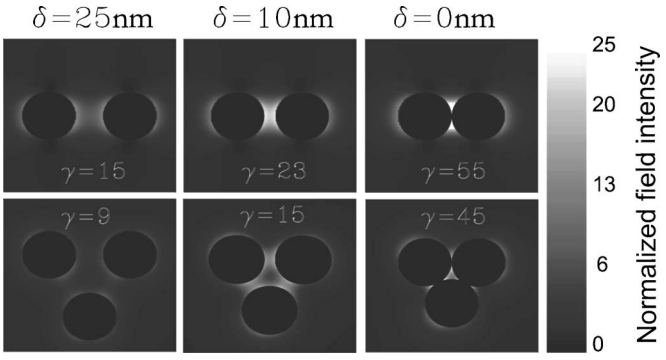

Fig. 4. Evolution of the local field intensity map ($\lambda = 550$ nm) around gold dimers (linear polarization) and trimers (circular polarization) for three different separation distances: $\delta = 25$ nm for the first column, $\delta = 10$ nm for the second column, and $\delta = 0$ nm for the third column. At each position, a normalization is done with respect to the incident intensity.

intensity we consider, MNPs can bind for $\delta = 380$ nm according to a trimer conformation while binding between only two particles is not expected to be strong enough.

At short distances ($\delta < 100$ nm), the strong attractive optical forces between MNPs trigger clustering.[4] Note that this effect may be assisted by van de Waals forces. A specificity of metal clusters is their ability to lead to a strong charge gradient in the air interstices resulting in intense and confined *hot spots*.[15] This is illustrated in Fig. 4 where the local field intensity distribution in the half-plane of the particles is mapped for dimers and trimers with different gap distances. At each point, a normalization is done with respect to the incidence. In both cases, the gap field intensity significantly increases and gets more localized when δ decreases. When getting in contact ($\delta = 0$ nm), the maximum field enhancement γ reaches 55 for dimers and 45 for trimers. These values are consistent with the significant enhancement of Raman signals (proportional to $|E|^4$) observed by Swedberg[7,8] and co-workers on ensembles of trapped metal nanoparticles and dimers. The dynamics of metal particles that we observe on assemblies of two and three MNPs can be generalized to a higher number of particles taking into account the continuous change of the resonance while increasing the system size.

This research was carried out with the financial support of the European Commission through grant ATOM3D FP6-508952 and the Network of Excellence "Plasmon Nano-devices" (PND)-507879. M. Nieto-Vesperinas acknowledges financial support from the EU and the Spanish Department of Scientific Research. R. Quidant's e-mail address is romain.quidant@icfo.es.

*Also with ICREA–Institució Catalana de Recerca i Estudis Avançats, 08010 Barcelona, Spain.

References

1. K. Svoboda and M. Block, Opt. Lett. **19**, 930 (1994).
2. P. M. Hansen, V. K. Bhatia, N. Harrit, and L. Oddershede, Nano Lett. **5**, 1937 (2005).
3. A. S. Zelenina, R. Quidant, G. Badenes, and M. Nieto-Vesperinas, Opt. Lett. **31**, 2054 (2006).
4. H. Xu and M. Käll, Phys. Rev. Lett. **89**, 246802 (2002).
5. K. Imura, H. Okamoto, M. K. Hossain, and M. Kitajima, Nano Lett. **6**, 2176 (2006).
6. S. Enoch, R. Quidant, and G. Badenes, Opt. Express **12**, 3422 (2004).
7. F. Svedberg, L. Zhipeng, X. Li, H. Xu, and M. Käll, Nano Lett. **6**, 2639 (2006).
8. F. Svedberg and M. Käll, Faraday Discuss. **132**, 35 (2006).
9. Y. Zhang, C. Gu, A. Schwartzberg, S. Chen, and J. Zhang, Phys. Rev. B **73**, 165405 (2006).
10. C. Chaumet, P. Nieto-Vesperinas, and M. Nieto-Vesperinas, Phys. Rev. B **61**, 14119 (2000).
11. S. Sburlan, L. A. Blanco, and M. Nieto-Vesperinas, Phys. Rev. B **73**, 035403 (2006).
12. I. Romero, J. Aizpurua, G. W. Bryant, and F. J. Garcia de Abajo, Opt. Express **14**, 9988 (2006).
13. P. C. Chaumet and M. Nieto-Vesperinas, Phys. Rev. B **64**, 035422 (2001).
14. S. Mohanty, J. Andrews, and P. Gupta, Opt. Express **12**, 2746 (2004).
15. C. Girard, E. Dujardin, M. Li, and S. Mann, Phys. Rev. Lett. **97**, 100801 (2006).